Supporting information

Chemical State Tuning of Surface Ce Species on Pristine CeO_2 with 2400% Boosting in Peroxidase-like Activity for Glucose Detection

Jieru Zhang,[a] Zicong Tan,[a] Wanying Leng,[a] Yu-Cheng Chen,[b] Shiqing Zhang,[c] Benedict T.W. Lo[d], Ken Kin Lam Yung[c] and Yung-Kang Peng[*a,e]

[a]Department of Chemistry, City University of Hong Kong, Hong Kong, China.

[b]Department of Mechanical Engineering, City University of Hong Kong, Hong Kong, China.

[c]Department of Biology, Hong Kong Baptist University, Hong Kong, China.

[d]Department of Applied Biology and Chemical Technology, Hong Kong Polytechnic University, Hong Kong, China.

[e]City University of Hong Kong Shenzhen Research Institute, Shenzhen 518057, China.

*Correspondence: ykpeng@cityu.edu.hk

EXPERIMENTAL SECTION

Materials.

Cerium (III) nitrate hexahydrate ($Ce(NO_3)_3 \cdot 6H_2O$, reagent grade, Sigma-Aldrich), hexamethylenetetramine (HMT, reagent grade, Sigma-Aldrich), Sodium hydroxide (reagent grade, Sigma-Aldrich), Sodium Acetate (CH_3COONa, Sigma-Aldrich), Acetic acid (AcOH, Sigma-Aldrich), Ethanol (absolute ≥ 99.8%, Sigma-Aldrich), Hydrogen peroxide solution (30 % (w/w) in H_2O, Sigma-Aldrich), 3,3‘,5,5’-Tetramethylbenzidine (TMB, Aladdin), Glucose (Sigma-Aldrich), Glucose oxidase (GOx, 145.2 kU g−1,Sigma-Aldrich), Human serum sample (Solarbio.), Fetal bovine serum (FBS)(Life technlolgies), Horse serum sample (Life technlolgies), Phosphate buffer solution (PBS, pH 7.0, 10X, J&K), Acetate buffer solution (pH=4.0) was prepared by AcOH and CH_3COONa, Water was purified by a Millipore Milli-Q System (resistivity is 18.2 MΩ·cm).

Synthesis of CeO_2 shapes.

CeO_2 octahedron was synthesized by mixing 1 mmol of $Ce(NO_3)_3 \cdot 6H_2O$ and 25 mmol of HMT in deionized water (50 mL) at 75 °C for 3 hours. Both rod and cube were prepared by heating the solution of $Ce(NO_3)_3$ and NaOH at 100°C and 180°C hydrothermally for 24 hours. 0.744g of $Ce(NO_3)_3 \cdot 6H_2O$ was mixed with 30 mL of 6 M NaOH solution for rod, while 0.6513g of $Ce(NO_3)_3.6H_2O$ was mixed with 30 mL of 3M NaOH solution for cube. All products were washed three times with deionized water and dried at 200 °C before use.

Peroxidase mimicking activity and Michaelis–Menten kinetic study.

The peroxidase mimicking reaction was initiated by mixing 25 μL CeO_2 solution (1.0 mg/mL), 0.3 mL TMB solution (10 mM), 2.375 mL acetate buffer (50 mM, pH=4.0) and 0.3 mL H_2O_2 solution (1 M). The final concentration of TMB and H_2O_2 were thus 1 mM and 0.1 M. To compare activity of CeO_2 shapes with similar surface area, the concentration of CeO_2 rod for this reaction was fixed at 1.0 mg/mL and the concentration for cube and octahedron can be calculated 3.3 mg/mL and 2.0 mg/mL according to the difference in their surface area. For Michaelis–Menten kinetic analysis, different concentration of substrates (H_2O_2 and TMB) were adopted to evaluate the corresponding affinity to CeO_2 shapes (see Figure S5). For H_2O_2, 0.3 mL H_2O_2 solution with different concentration (0.01, 0.02, 0.05, 0.1, 0.2, 0.5, 1, 2 M) was pre-mixed with 0.3 mL TMB solution (10 mM) and 2.375 mL acetate buffer (50 mM, pH=4.0) before adding 25 μL CeO_2 solution (1 mg/mL). The final concentration of H_2O_2 was 0.01, 0.02, 0.05, 0.1, 0.2, 0.5, 1, 2 M respectively. Similar for TMB, 0.3 mL TMB solution with different concentration (0.1, 0.2, 0.5, 1, 2, 5, 10, 20 mM) was pre-mixed with 0.3 mL H_2O_2 solution (0.1 M) and 2.375 mL acetate buffer (50 mM, pH=4.0) before adding 25 μL CeO_2 solution (1 mg/mL). The final concentration of TMB was 0.01, 0.02, 0.05, 0.1, 0.2, 0.5, 1, 2 mM respectively. The Michaelis constant (K_m) and the maximum reaction velocity (V_{max}) can be obtained by the equation below:

$$V = V_{max} \frac{[S]}{([S] + K_m)}$$

Where V is the initial speed, V_{max} is the maximum reaction speed, [S] is the concentration of H_2O_2 or TMB, and K_m is the corresponding Michaelis constant. Measurements were recorded by UV-Vis every 6 second at room temperature. The initial reaction rate V_0 was calculated from the first 5 minutes of the reaction.

H_2O_2 and glucose detection.

For H_2O_2 detection, H_2O_2 solution with different concentration (0.01, 0.02, 0.03, 0.04, 0.05, 0.075, 0.1, 0.2, 0.5, 1, 2, 3 mM) was firstly prepared. 300 μL H_2O_2 solution was pre-mixed with 300 μL TMB

solution (20 mM) and 2.35 mL acetate buffer (50 mM, pH=4.0). The reaction was carried out at 37 °C and initiated by adding 50 μL CeO_2 solution (1 mg/mL). The final concentration of H_2O_2 was 1, 2, 3, 4, 5, 7.5, 10, 20, 50, 100, 200, 300 μM respectively. UV-vis was used to record the generation of TMB_{ox} at 652 nm after 20 min of reaction. For glucose detection, glucose solution with different concentration (0.01, 0.02, 0.03, 0.04, 0.05, 0.075, 0.1, 0.2, 0.5, 1, 2, 3 mM) was also prepared first. 300 μL of this solution with different concentration was allowed to react with 50 μL GOx (10 mg/mL) for 30 minutes at 37 °C (denoted as solution A). Solution B was individually prepared by mixing 300 μL TMB solution (20 mM), 2.3 mL acetate buffer (50 mM, pH=4.0) and 50 μL CeO_2 solution (1 mg/mL). Solution A was then mixed with solution B for another 20 minutes at 37 °C. The final concentration of glucose was 1, 2, 3, 4, 5, 7.5, 10, 20, 50, 100, 200, 300 μM respectively. UV-vis was also used to record the generation of corresponding TMB_{ox} at 652 nm. The limit of detection (LOD) was calculated using the formula: LOD = 3 (SD / B), where B and SD represent the slope of the resulting calibration curve and the corresponding standard deviation of y-intercept.[1]

Selectivity test.

300 μL of ascorbic acid, cysteine, agarose, sucrose, D-sorbitol and glutathione solution was individually prepared (5 mM) for selectivity test. 300 μL of each solution was mixed with 50 μL GOx (10 mg/mL) and incubated at 37 °C for 30 minutes. The solution was then mixed with solution B prepared above and allowed to react at 37 °C for another 20 minutes. UV-vis was used to record the generation of corresponding TMB_{ox} at 652 nm. Note that the result of 1 mM glucose solution was compared in Figure 4e.

Glucose detection in serum samples.

Each serum sample was diluted 10 times by PBS buffer before use. 150 μL serum sample was mixed with 50 μL GOx (10 mg/mL) and incubated at 37 °C for 30 minutes. This solution was then mixed with solution B prepared above and allowed to react at 37 °C for another 20 minutes. UV-vis was used to record the generation of corresponding TMB_{ox} at 652 nm.

Linear sweep voltammetry (LSV) measurement.

LSV measurement was carried out by CHI650E Electrochemistry Workstation using Ag/AgCl as reference electrode and a Pt wire as counter electrode. The glass carbon electrode (GCE) (working electrode) was prepared by mixing 2 mg CeO_2 with a conductive polymer Nafion (50 μL; 5 wt%) in 0.45 mL solvent (ethanol : H_2O = 1 : 1)

Raman spectroscopy measurement.

BaySpec's Agility™ Raman spectrometer using an excitation laser wavelength of 785 nm was employed for the monitoring of H_2O_2 activation. The H_2O_2 solution (6 mM) was firstly prepared using acetate buffer (pH = 4.0, 0.5 M) and 30% H_2O_2. For Raman measurement, 3 mg of CeO_2 (cube/octahedron) was loaded on a clean glass slide in 2 mm*2 mm area. The corresponding Raman spectrum obtained from raw ceria was set as 0 min. The spectra were also recorded at 1, 4, 10, 15 and 30 min after the adding 10 μL of H_2O_2 solution on ceria.

^{31}P NMR measurement.

The surface of CeO_2 sample (150 mg) was firstly cleaned at 373 K under vacuum (10^{-1} Pa) for 2 h before trimethylphosphine (TMP) adsorption in a glass vial. Around 300 μmol/catalyst g of TMP was then introduced to the sample vial and allowed to reach equilibrium for 15 minutes. The ^{31}P NMR measurement (Bruker Avance III 400WB) was carried out at room temperature. The ^{31}P chemical shifts were calibrated relative to 85% aqueous solution of H_3PO_4. The quantitative analysis of adsorbed

TMP molecules was then calculated according to the ^{31}P calibration line established in our previous literatures.[2, 3]

Density functional theory (DFT) calculation.

The DFT calculation of CeO_2 surfaces were carried out on the Vienna *ab initio* simulation package,[4] with projector augmented wave (PAW).[5] We introduced the on-site Coulomb interactions (DFT+U) correction, effective Hubbard U of 3 eV to the Ce(4f) states,[6] to obtain a better understanding of the geometric and electronic structures of CeO_2 surface. The lattice parameter of bulk CeO_2 was optimized with *k*-point sampling of 7 × 7 × 7 led to a lattice constant of 5.51 Å that is consistent with the experimental value of 5.41 Å.[7] CeO_2 surfaces were constructed as a slab within the three-dimensional periodic boundary conditions. This model was separated from their periodic images in the z direction perpendicular to the surface by a vacuum layer more than 14 Å. The slab systems were constructed from bulk parameters, the bottom three layers were fixed and the rest layers were allowed relax. The electron density of surface unsaturated Ce atom ($\rho_{surf.}$) can be obtained from the optimized CeO_2 surfaces. This value was further compared with the electron density of their 8-coordinated counterpart in bulk (ρ_{bulk}) by equation: $\Delta\rho = \rho_{surf.} - \rho_{bulk}$. Since the ρ_{bulk} of Ce is a fixed constant, the magnitude of $\Delta\rho$ is thus proportional to the corresponding ρ_{surf} of Ce for a given CeO_2 surface as plotted in the middle row of Figure 1. Similar methodology has been adopted by Chen et al. to visualize the electron density contours of platinum trimer on cobalt-palladium core-shell nanocatalyst.[8]

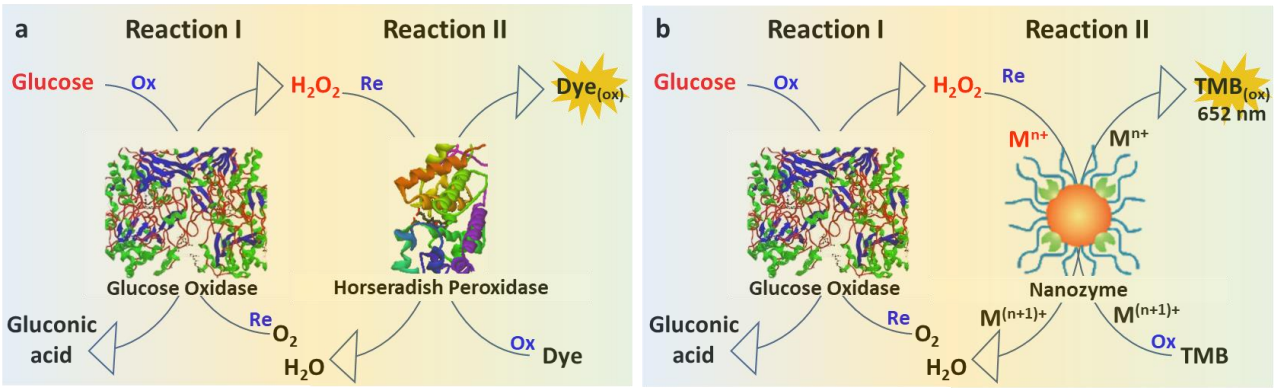

Scheme S1. The working principle of the colorimetric assay for glucose detection: (a) Conventional "enzymatic assay" using Horseradish peroxidase (HRP) as the second enzyme. (b) Using artificial nanozyme to mimic HRP in the second enzymatic reaction of glucose detection (TMB: tetramethylbenzidine).

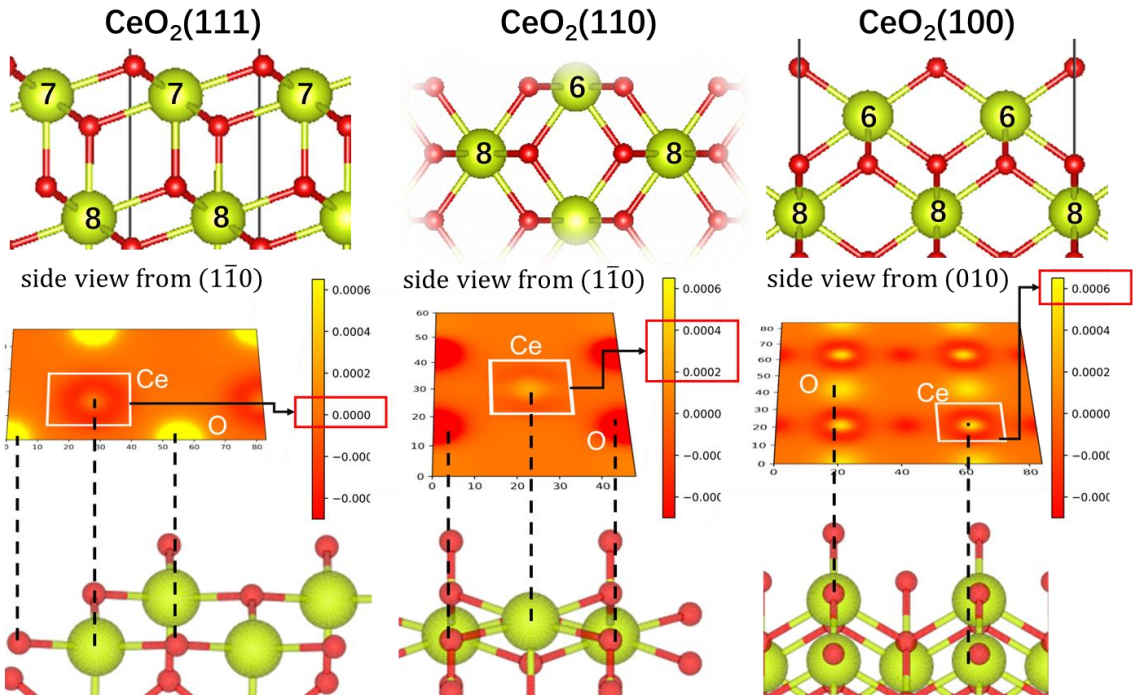

Scheme S2. Surface crystallographic $CeO_2(111)$, $CeO_2(110)$ and $CeO_2(100)$ structures. The number labelled on the Ce atom shows its coordination number. Middle row: the difference in electron density between saturated Ce in bulk (8 coordination) and surface unsaturated Ce on CeO_2 facets. Noted that the electron density of 7-coordinated Ce on CeO2(111) was set at 0.0000 for comparison.

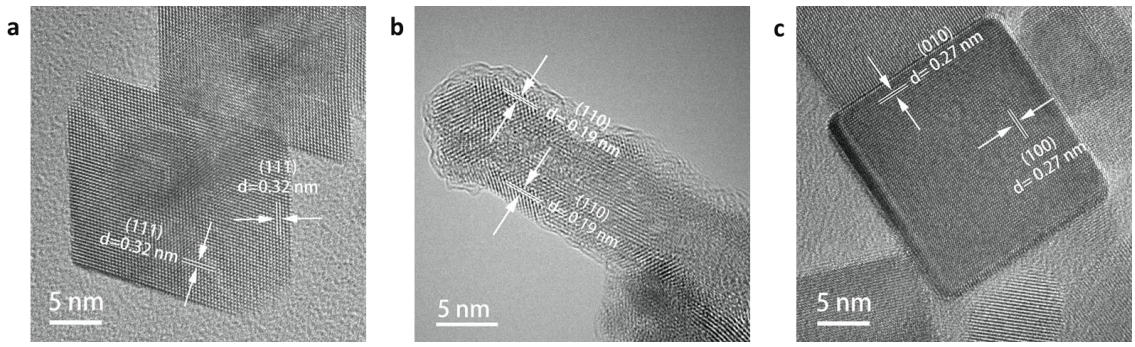

Figure S1. High-resolution TEM (HRTEM) images of CeO_2 (a) octahedron, (b) rod and (c) cube.

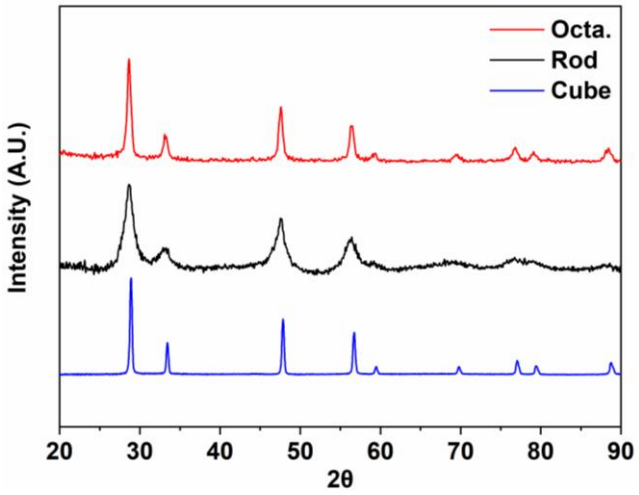

Figure S2. XRD patterns of the CeO_2 morphologies indexed to JCDPS no. 65-2795 for CeO_2 with a fluorite type of crystal structure.

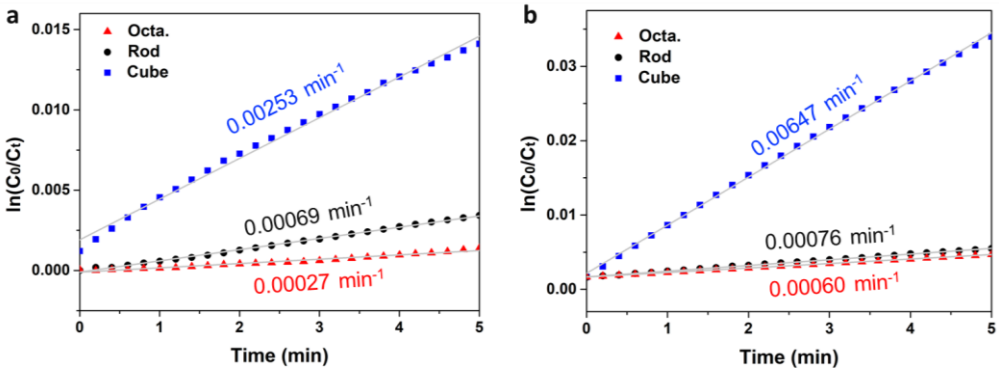

Figure S3. First order fitting of peroxidase mimicking activity over CeO_2 shapes with same tested (a) weight (i.e. 1 mg for each shape), (b) surface area (i.e. 2 mg for octahedron, 1 mg for rod and 3.3 mg for cube).

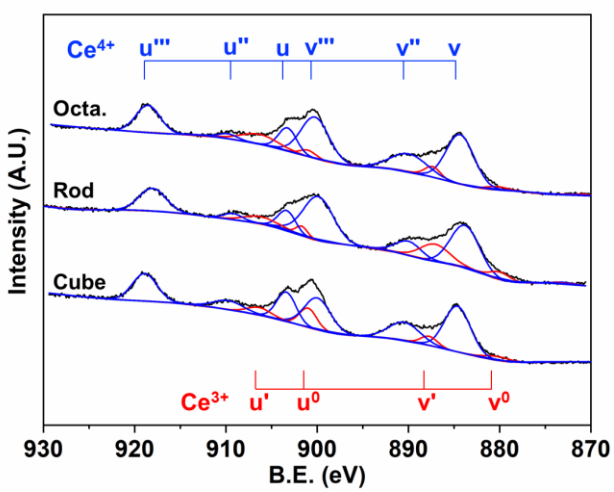

Figure S4. Deconvoluted XPS Ce_{3d} results of CeO_2 shapes. The binding energy 284.6 eV of C_{1s} was taken as the standard to calibrate all the XPS spectra. All Ce_{3d} XPS spectra were recorded by a Thermo XPS equipped Al as X-ray source.

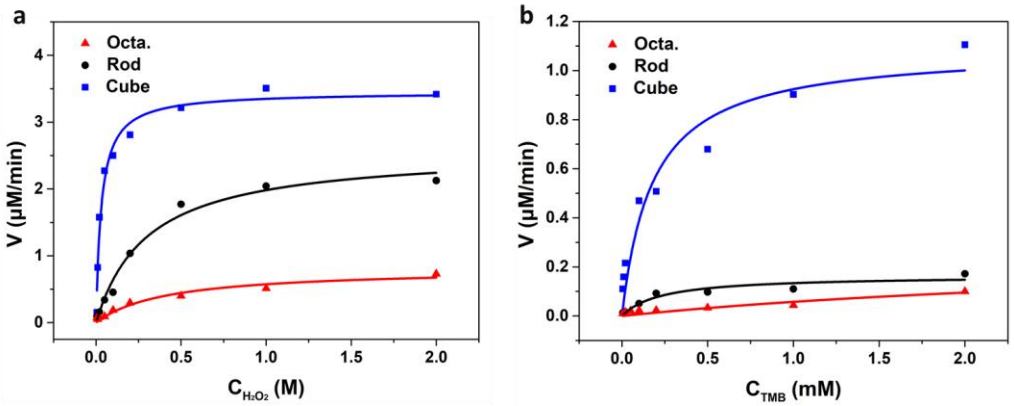

Figure S5. Steady-state Michaelis-Menten study of CeO_2 shapes with various concentration range for (a) H_2O_2 (1 mM TMB was used) and (b) TMB (0.1 M H_2O_2 was used). See Table S1 for corresponding Michaelis–Menten constant (K_m) and maximum reaction rate (V_{max}).

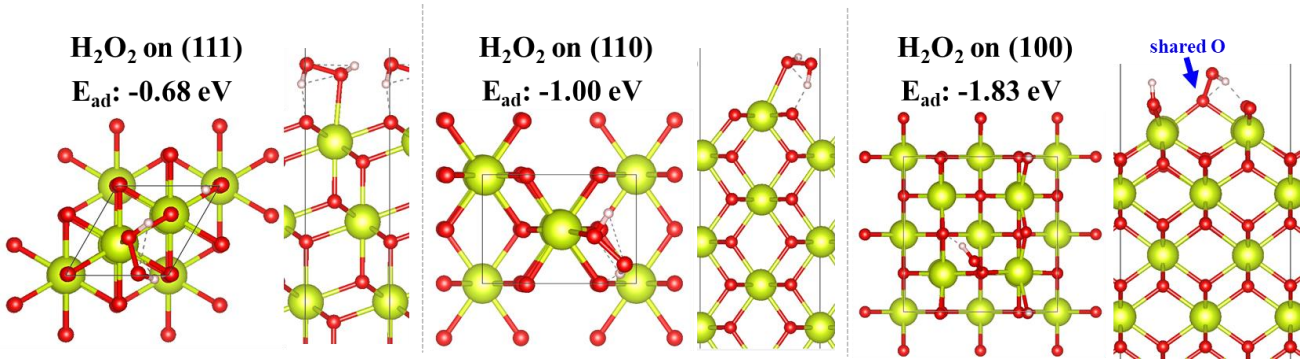

Figure S6. H_2O_2 adsorption configuration on CeO_2 (111), (110), (100) facets and corresponding adsorption energy.

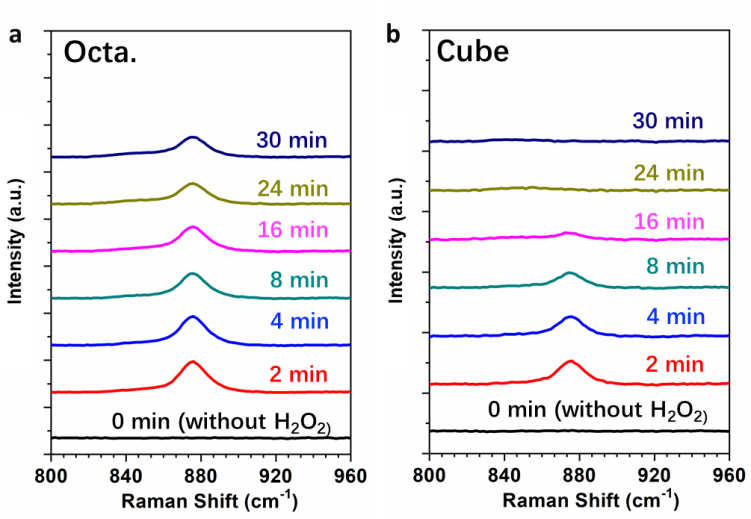

Figure S7. Time-dependent *in-situ* Raman spectra of CeO_2 (a) octahedron and (b) cube in the presence of H_2O_2.

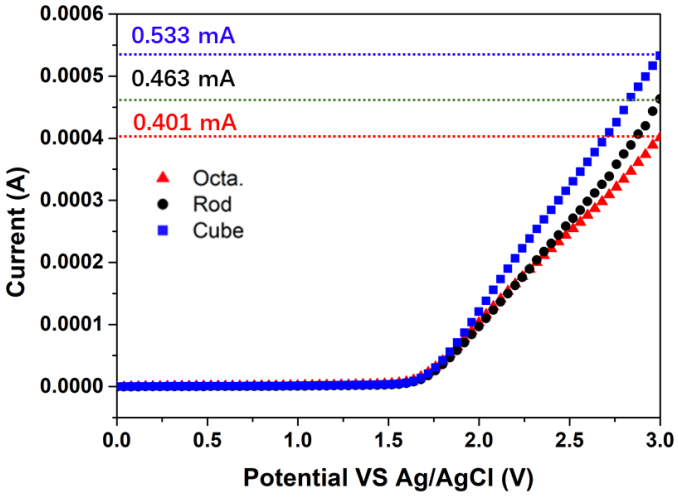

Figure S8. Linear sweep voltammetry (LSV) results of CeO_2 shapes. It is clearly that the cube shows higher current than the other two shapes when the applied voltage is higher than 1.75 V (vs Ag/AgCl). For example, the highest current can be found on the cube (0.533 mA) followed by the rod (0.463 mA) and octahedron (0.401 mA) when the applied voltage is fixed at 3V. This result again supports our finding that the electron density of surface Ce is shape-dependent in the order of cube (100) > rod (110) > octahedron (111).

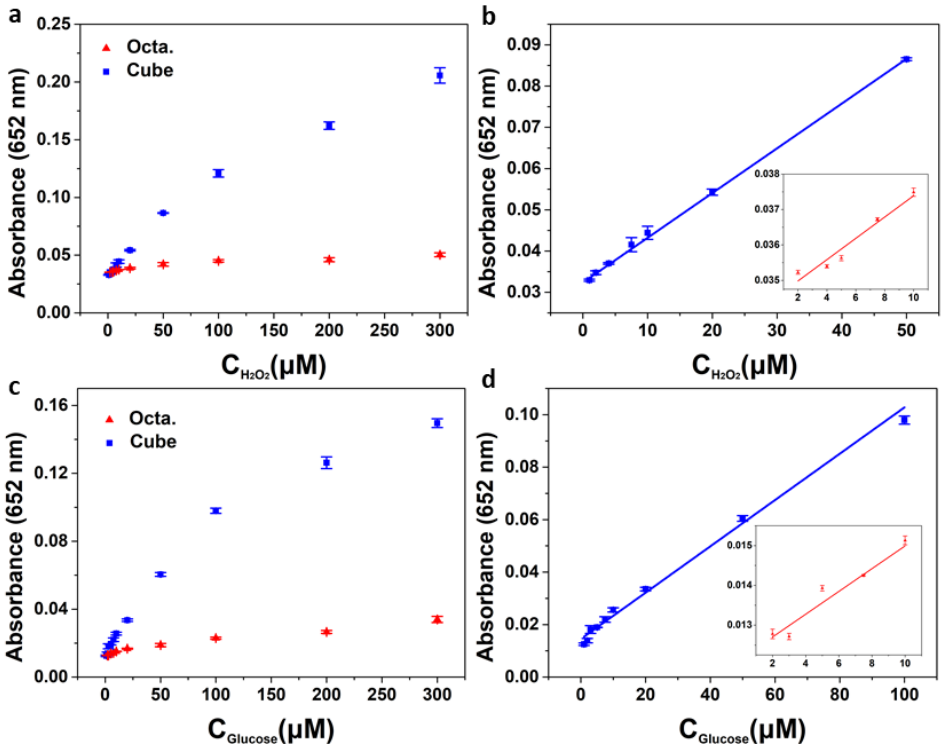

Figure S9. The calibration curves and linear plots for (a, b) H_2O_2 and (c, d) glucose detection using CeO_2 shapes as peroxidase mimetics (same weight of catalyst was used). Note that all error bars in this figure show the standard deviations of three replicates.

Table S1. General information of CeO_2 shapes including terminal facet, surface area, Ce^{3+}/Ce^{4+} ratio and the acidity of surface Ce and corresponding concentration.

	exposed facet	$S_{BET}(m^2g^{-1})$	Ce^{3+}/Ce^{4+} ratio	Ce acidity ($\delta^{31}P$)	$[Ce]_{surface}$ (μmol/g)
Octa.	(111)	46	0.15	-33	0.54
Rod	(110)	95	0.25	-47.5	0.37
Cube	(100)	29	0.18	-58	0.21

Table S2. Michaelis–Menten constant (K_m) and maximum reaction rate (V_{max}) of H_2O_2 and TMB among CeO_2 morphologies.

	H_2O_2		TMB	
	K_m (M)	V_{max} (μM/min)	K_m (mM)	V_{max} (μM/min)
Octa.	0.4152	0.8163	3.7430	0.2736
Rod	0.3020	2.5813	0.2302	0.1646
Cube	0.0309	3.4521	0.1801	1.0904

Table S3. Comparison of Michaelis–Menten constant (K_m) and maximum reaction rate (V_{max}) for different metal oxide nanozyme.

Catalyst	Substrate	K_m(mM)	V_{max} (μM/ min)	Reference
Fe_3O_4 NPs	H_2O_2	154	5.868	9
	TMB	0.098	2.064	
CeO_2 NPs	H_2O_2	64.6	3.042	10
	TMB	0.046	0.564	
CuO NPs	H_2O_2	41	N/A	11
	TMB	0.016	N/A	
Co_3O_4 NPs	H_2O_2	140.07	7.26	12
	TMB	0.037	7.762	
CeO_2 Octa.	H_2O_2	415.2	0.8163	This work
	TMB	3.743	0.2736	
CeO_2 Rod	H_2O_2	302	2.5813	This work
	TMB	0.230	0.1646	
CeO_2 Cube	H_2O_2	30.9	3.4521	This work
	TMB	0.1801	1.0904	

Discussion on Table S3: Among CeO_2 shapes, H_2O_2 and TMB both exhibit the highest affinity to cube followed by rod and octahedron with increasing K_m value. Even though the rod shows similar TMB K_m (0.203 mM) as that of the cube (0.1801 mM), its low peroxidase-like activity can be attributed to the low H_2O_2 affinity of rod surface (same as the octahedron). This result thus suggests that the affinity of H_2O_2 to nanozyme is the key step dictating its mimicking activity rather than that of TMB. Similar explanation can be extended to other metal oxides such as Fe_3O_4, Co_3O_4 and CuO listed in Table S3. Although CeO_2 cube has the lowest TMB affinity (i.e. the highest in TMB K_m) among them, its highest H_2O_2 affinity (i.e. the lowest in H_2O_2 K_m) suggests that CeO_2 cube can be the best candidate as peroxidase mimetics among the listed metal oxides.

Table S4. The fitting result of targets detection.

Nanozyme	Target	Slope (10^{-4})	SD (10^{-4})[a]	R-square	Linear range	LOD (μM)[b]
CeO_2 Octa.	H_2O_2	3.01	2.578	0.915	2-10 μM	2.569
	Glucose	2.86	3.394	0.897	2-10 μM	3.557
CeO_2 Cube	H_2O_2	10.8	1.952	0.999	1-50 μM	0.542
	Glucose	8.83	4.595	0.983	1-100 μM	0.904

[a]SD= standard deviation. [b]LOD= Limit of detection.

Table S5. Target detection of different peroxidase mimics using colorimetry method.

Nanozyme	Target	Linear range	LOD	Reference
CeO_2 NPs	H_2O_2	0.5-1.5 μM	0.5 μM	10
	Glucose	6.6-130 μM	3 μM	
Co_3O_4 NPs	H_2O_2	0.05-25 mM	10 μM	12
	Glucose	0.01-10 mM	5 μM	
Fe_3O_4 MNPs	H_2O_2	5-100 μM	3 μM	13
	Glucose	50-1000 μM	30 μM	
CeO_2 Octa.	H_2O_2	2-10 μM	2.569 μM	This work
	Glucose	2-10 μM	3.557 μM	
CeO_2 Cube	H_2O_2	1-50 μM	0.542 μM	This work
	Glucose	1-100 μM	0.904 μM	

Table S6. Results of glucose level in serum samples determined by commercial glucose assay kit (method A, Scheme 1a) and using CeO_2 cube as peroxidase mimetics (method B, Scheme 1b). The relative standard deviation (RSD) was obtained by dividing the standard deviation by the corresponding average value.

	Method A (mM)[a]	RSD (%)	Method B (mM)[b]	RSD (%)	Recovery (%)[c]
Serum1	1.13 ± 0.06	5.30	1.02 ± 0.04	3.92	90.3
Serum2	2.06 ± 0.12	5.83	2.15 ± 0.16	7.44	104.3
Serum3	3.90 ± 0.10	2.56	4.01 ± 0.18	4.49	102.8

[a]The glucose level determined by the commercial glucose assay kit (method A, Scheme 1a).
[b]The glucose level determined by using CeO_2 cube as peroxidase mimetics (method B, Scheme 1b).
[c]Recovery was calculated by dividing the averaged concentration obtained in method B by method A.

References:

1 Nirala, Narsingh R, *Sens. Actuators B Chem.* 2015, **42**, 218.

2 Y.-K. Peng, L. Ye, J. Qu, L. Zhang, Y. Fu, I. F. Teixeira, I. J. McPherson, H. He, S. C. E. Tsang, *J. Am. Chem. Soc.* 2016, **138**, 2225–2234.

3 Y.-K. Peng, Y. Hu, H.-L. Chou, Y. Fu, I. F. Teixeira, H. He, S. C. E. Tsang, *Nat. Commun.* 2017, **8**, 675.

4 G. Kresse, J. Furthmüller, *Phys. Rev. B* 1996, **54**, 11169.

5 G. Kresse, D. Joubert, *Phys. Rev. B* 1999, **59**, 1758.

6 C. Loschen, J. Carrasco, K. M. Neyman, F. Illas, *Phys. Rev. B* 2007, **75**, 035115.

7 E. A Kümmerle, G Heger, *J. Solid State Chem.* 1999, **147**, 485−500.

8 S. Dai, J.-P. Chou, K.-W. Wang, Y.-Y. Hsu, A. Hu, X. Pan, T.-Y. Chen, *Nat. Commun.* 2019, **10**, 440.

9 L. Gao, J. Zhuang, L. Nie, J. Zhang, Y. Zhang, N. Gu, T. Wang, J. Feng, D. Yang, S. Perrett, X. Yan, *Nat. Nanotechnol.* 2007, **2**, 577−583.

10 X. Jiao, H. Song, H. Zhao, W. Bai, L. Zhang, Y. Lv, *Anal. Methods.* 2012, **4**, 3261−3267.

11 W. Chen, J. Chen, Y.-B. Feng, L. Hong, Q.-Y. Chen, L.-F. Wu, X.-H. Lin, X.-H. Xia, *Analyst.* 2012, **137**, 1706−1712.

12 J. Mu, Y. Wang, M. Zhao, L. Zhang, *Chem. Commun.* 2012, **48**, 2540−2542.

13 H. Wei, E. Wang, *Anal. Chem.* 2008, **80**, 2250−2254.